Mechanical/Control Integrated Design of a Flexible Planar Rotatory Spacecraft

J.A. Perez, D. Alazard, T. Loquen and C. Pittet

1 Introduction

Currently Large Space Structures (LSS) are a challenging problem in control system design because they involve large complex kinematic chains composed of rigid and flexible bodies, mostly large-sized, maximally lightened, low-damped and with closed-spaced low natural frequencies. In this case structural modes interfere the controlled bandwidth, provoking a critical Control-Structure Interaction (CSI). Therefore, LSS design is increasingly becoming subject to a close coordination among the different spacecraft sub-systems, demanding methods which tie together spacecraft structural dynamics, control laws and propulsion design. These methods are often called as *Integrated Control/Structure Design* (ICSD), *Plant-Controller Optimization* (PCO) or simply *co-design* (CD).

ICSD methods began being studied in the 80 s as an opposite technique to the current method of separated iterative sequences within the structural and control disciplines. The first integrated design methodologies were those in [1–3]. These methods were based on iterative methodologies with optimization algorithms. Lately, other methods have been proposed such as those solved by LMI (Linear Matrix Inequality) algorithms or with LQG (Linear Quadratic Gaussian) methods like in [4, 5] respectively. However, these approaches give conservative results and their applicability is restricted by problem dimension. Recently, a counterpart technique currently under development in ONERA Toulouse Research Center and ISAE-SUPAERO allows a

J.A. Perez (✉) · T. Loquen
ONERA, 2 Avenue Edouard Belin, 31055 Toulouse, France
e-mail: Jose-Alvaro.perez_gonzalez@onera.fr

T. Loquen
e-mail: thomas.loquen@onera.fr

D. Alazard
ISAE, 10 Avenue Edouard Belin, 31055 Toulouse, France
e-mail: daniel.alazard@isae.fr

C. Pittet
CNES, 18 Avenue Edouard Belin, 31400 Toulouse, France
e-mail: christelle.pittet@cnes.fr

B. Dołęga et al. (eds.), *Advances in Aerospace Guidance, Navigation and Control*, https://doi.org/10.1007/978-3-319-65283-2_35

more general approach [6]. Actually, this method is based on structured $\mathscr{H}_\infty$ synthesis algorithms developed in [7] or [8], granting structured controllers and tunable parameters optimization. This synthesis, merged with a correct plant modeling, can reveal important applications of integrated design methodologies.

To be compliant with such an ICSD approach, the plant modeling of LSS must provide a model where the structural or mechanical sizing parameters can be isolated under the general Linear Fractional Representation (LFR). That can be performed using the Two-Input Two-Output Port (TITOP) approach to build the linear dynamical model of Flexible Multi-body System (FMS) from the model of each body. The TITOP model approach was first proposed in [9], then generalized to take into account varying sizing parameters in [10, 11]. For uniform beam, an analytic model was developed in [12] where a first ICSD was presented. Augmented TITOP models for flexible body actuated with piezoelectric strip [13] involve an additional channel between the input voltage and the output piezoelectric charge, allowing any active substructure to be embedded in the whole structure. Some applications of ICSD using such a modeling technique are presented in [14, 15].

This work aims at showing the way to apply these modeling and design tools to perform the ICSD of a flexible planar rotatory spacecraft. Such a system was presented in [16] to illustrate interactions between control and structure in space engineering. The objective is to maximize the length and the tip mass of one appendage, in order to increase the spacecraft payload capacity, while minimizing the total mass of the spacecraft and meeting attitude pointing requirement in spite of external disturbances. This paper is organized as follows. First, the parametric model of the spacecraft is developed. Second the integrated control design is presented. Finally, results and discussion on advantages of using this methodology rather than single control optimization alone are detailed.

2 Flexible Rotatory Spacecraft Modeling

2.1 Spacecraft System Description

The system, considered as an academic example, is composed of a rigid main hub with four identical cantilevered flexible appendages and tip masses as shown in Fig. 1. The configuration parameters are provided in Table 1. Under normal operation, the spacecraft undergoes planar rotational maneuvers around the inertial fixed axis **z**. The spacecraft body frame is attached to the center of mass of the rigid hub, and it is denoted by a right-handed triad **x**, **y** and **z**. The rotation about the axis **z** is denoted by the angle θ and the translational deformation of each tip by w^i_{tip}, with superscript i denoting the beam number.

The system is actuated by three different torques. The main torque, t_{hub} is provided by the main hub about the axis **z**. Two additional input torques, $t_{tip,1}$ and $t_{tip,2}$, are applied at the tip masses 1–3 and 2–4 respectively. These torques can be applied

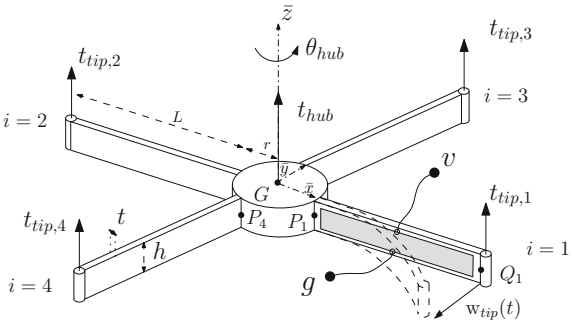

Fig. 1 Rotatory flexible spacecraft

Table 1 Spacecraft configuration parameters

Parameters	Symbol	Value
Hub radius	r	0.31 m
Hub mass	m_h	233.50 kg
Hub inertia	J_h	10.85 kg/m^2
Beam mass density	ρ	1.30 kg/m
Beam elastic modulus	E	75.84 GPa
Beam length	L	1.22 m
Beam thickness	t	3.18 mm
Beam height	h	0.15 m
Tip mass	m_t	2.29 kg
Tip mass inertia	J_t	2.44 g/m^2
Nodes beam FEM	nod	11
Number of AM	asm	13
Piezo parameters	Symbol	Value
Thickness	t_p	2 mm
Width	w_p	30 mm
Volumetric density	ρ_p	7600 kg/m^3
Elastic modulus	E_p	50 GPa
Piezoelectric constant	d_{31}	-150×10^{-12} m/V
Dielectric constant	ε_{33}^T	1.59×10^{-12} F/m

purposely for control reasons or can represent environment disturbances (as it is the case in this paper). In addition, the appendage # 1 is actuated using a piezoelectric strip for active damping of vibrations.

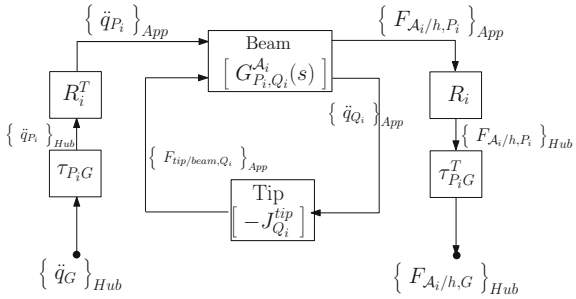

Fig. 2 Model $A_i(s)$ of a single appendage ($i = 2, 3, 4$)

2.2 Spacecraft System Modeling

The whole spacecraft is decomposed in various sub-structures: the hub h and the 4 appendages $\mathscr{A}_i, i = 1, \ldots, 4$. Each appendage is itself decomposed into a uniform beam which flexible dynamics is represented by a super-element [11] and a local mass/inertia at the tip of the beam. The TITOP (Two-Input Two-Output) model approach is used to described each sub-structure. The block diagram representation of a single appendage model is depicted in Fig. 2 where:

- $G^{\mathscr{A}_i}_{P_i,Q_i}(s)$ is the planar TITOP model of the flexible uniform beam # i (see [11] for more details): the inputs are the time-derivative of the planar twist $\ddot{q}_{P_i}$ (3 components: 2 linear accelerations and 1 angular acceleration) at point P_i of the beam and the external planar wrench $F_{tip/beam,Q_i}$ (3 components: 2 forces and 1 torque) applied to the beam at point Q_i. The output are the wrench $F_{\mathscr{A}_i/h,P_i}$ applied by the appendage to the hub at point P_i and the time-derivative of the twist $\ddot{q}_{Q_i}$ at point Q_i,
- $J^{tip}_{Q_i}(s)$ is the planar dynamical model of the tip mass and inertia:

$$J^{tip}_{Q_i} = \begin{bmatrix} m_t & 0 & 0 \\ 0 & m_t & 0 \\ 0 & 0 & J_t \end{bmatrix} \tag{1}$$

- τ_{P_iG} is the kinematic models between points G and P_i. In the planar case:

$$\tau_{P_1G} = \begin{bmatrix} 1 & 0 & 0 \\ 0 & 1 & r \\ 0 & 0 & 1 \end{bmatrix} \quad \tau_{P_2G} = \begin{bmatrix} 1 & 0 & 0 \\ 0 & 1 & -r \\ 0 & 0 & 1 \end{bmatrix} \quad \tau_{P_3G} = \begin{bmatrix} 1 & 0 & -r \\ 0 & 1 & 0 \\ 0 & 0 & 1 \end{bmatrix} \quad \tau_{P_4G} = \begin{bmatrix} 1 & 0 & r \\ 0 & 1 & 0 \\ 0 & 0 & 1 \end{bmatrix} \tag{2}$$

- R_i is the rotation matrix written as follows:

$$R_i = \begin{bmatrix} \cos\beta_i & -\sin\beta_i & 0 \\ \sin\beta_i & \cos\beta_i & 0 \\ 0 & 0 & 1 \end{bmatrix}_{App \to Hub} \tag{3}$$

where β_i is the angle of the ith appendage i with $\mathbf{x}$.

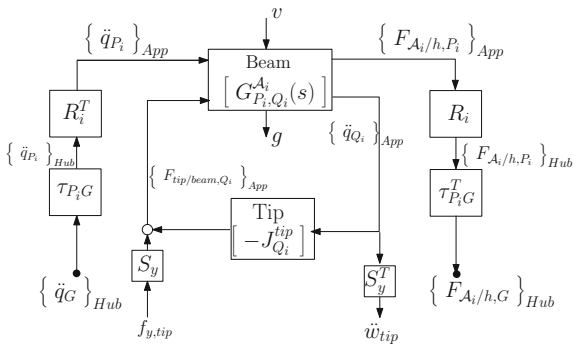

Fig. 3 Model $A_1(s)$ of appendage # 1 $i = 1$)

For the appendage # 1, actuated with a piezoelectric strip, the extension of TITOP model described in [13] is used. The augmented model $A_1(s)$ involves an additional channel between v (input voltage) and g (output piezoelectric charge). Furthermore a radial disturbance force $f_{y,tip}$ on input and the radial acceleration $\ddot{w}_{tip}$ on output are included to shape the control problem (see Sect. 3.2). For appendage $\mathscr{A}_1$, the model is then described in Fig. 3 where $S_y = [0 \quad 1 \quad 0]^T$.

The assembly of the various sub-models is described by the block diagram scheme presented in Fig. 4, where:

- $J_G^{Hub} = \begin{bmatrix} m_h & 0 & 0 \\ 0 & m_h & 0 \\ 0 & 0 & J_h \end{bmatrix}$
- $S_z = [0 \quad 0 \quad 1]^T$

The inputs and the outputs of the whole system mechanical model $(J_G^{sat})^{-1}(s)$ are:

- a vector w of two exogenous inputs: a disturbance $w_{\ddot{\theta}_{out}}$ on the hub angular acceleration and $f_{y,tip}$,
- a vector u of two control signals: the torque on the hub t_{hub} and the piezo input voltage v,
- a vector z of two controlled outputs: the hub angular rate $\ddot{\theta}_{hub}$ and the lateral tip acceleration $\ddot{w}_{tip}$ of appendage 1,
- a vector y of 3 measurements: the hub angular rate $\dot{\theta}_{hub}$ and attitude θ_{hub} and the lateral tip acceleration $\ddot{w}_{tip}$ of appendage 1.

2.3 *Spacecraft Model with Varying Parameters*

The structured model $(J_G^{sat})^{-1}(s)$ of the spacecraft is quite convenient to take into account some sizing mechanical parameters or design parameters. In this application,

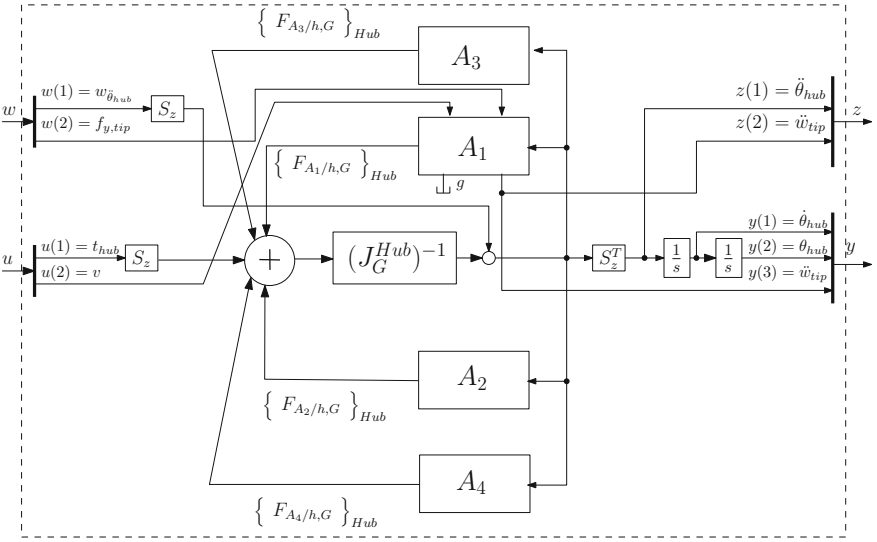

Fig. 4 Rotatory flexible spacecraft $(J_G^{sat})^{-1}(s)$

the design parameters are the length L_i and the tip mass M_i of each appendage. More precisely:

$$L_i = L(1 + 0.3\delta_{L_i}), \quad M_i = m_t(1 + 0.3\delta_{M_i}), \quad i = 1, 2, 3, 4.$$

That is to say: 30% of variations around the nominal value are allowed for each design parameters L_i and M_i in such a way that δ_{L_i} and δ_{M_i} are normalized to vary between -1 and 1. These design can be very easily isolated in the various submodels (L_i in $G^{\mathscr{A}_i}_{P_i,Q_i}(s)$ and M_i in $J^{tip}_{Q_i}$). Thus, using LFR for each parameters and basic LFR operations, one can easily derived the LFR of the whole spacecraft depicted in Fig. 5, also written:

$$(J_G^{sat})^{-1}(s, \delta_{L_1}, \delta_{L_2}, \delta_{L_3}, \delta_{L_4}, \delta_{M_1}, \delta_{M_2}, \delta_{M_3}, \delta_{M_4}) = F_u((M_G^{sat})^{-1}(s), \Delta) \ .$$

After assembly, the system has a block Δ of 125×125 size and reads:

$$[\Delta] = \begin{bmatrix} [\delta_{L_1}]_{30\times30} & 0 & 0 & 0 & 0 & 0 & 0 & 0 \\ 0 & [\delta_{M_1}]_{2\times2} & 0 & 0 & 0 & 0 & 0 & 0 \\ 0 & 0 & [\delta_{L_2}]_{29\times29} & 0 & 0 & 0 & 0 & 0 \\ 0 & 0 & 0 & [\delta_{M_2}]_{2\times2} & 0 & 0 & 0 & 0 \\ 0 & 0 & 0 & 0 & [\delta_{L_3}]_{29\times29} & 0 & 0 & 0 \\ 0 & 0 & 0 & 0 & 0 & [\delta_{M_3}]_{2\times2} & 0 & 0 \\ 0 & 0 & 0 & 0 & 0 & 0 & [\delta_{L_4}]_{29\times29} & 0 \\ 0 & 0 & 0 & 0 & 0 & 0 & 0 & [\delta_{M_4}]_{2\times2} \end{bmatrix} \tag{4}$$

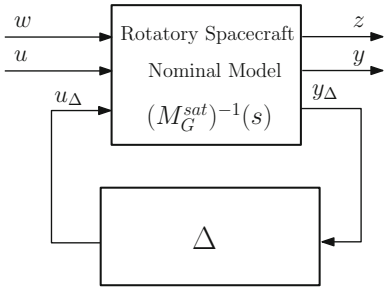

Fig. 5 Rotatory flexible spacecraft model with varying design parameters

That is: 2 parameter occurrences for each tip mass, 29 parameter occurrences for the non-actuated appendage lengths and 30 parameter occurrences for the actuated appendage length $i = 1$. The system results in a state-space system with a Δ block of size 125×125, 11 inputs, 11 outputs and 50 states.

It should be highlighted that the ICSD of the rotatory spacecraft strongly demands a modeling technique such as the TITOP modeling technique, since the boundary conditions of the flexible beams are to be changed when varying the mass located at their tips. Thus, by using the TITOP modeling technique, the impact of mass variation in the whole system will be taken into account when ICSD is performed with structured $\mathscr{H}_\infty$ synthesis. Indeed, in the symmetric nominal parametric configuration ($\Delta = 0$), some flexible modes are uncontrollable from u. Then, the damping of these flexible modes, when excited by a disturbance (on $f_{y,tip}, t_{tip,1}$ or $t_{tip,3}$), is not possible. The asymmetry introduced by the ICSD will restore the controllability and will allow active damping of all the modes, as it will be seen in Sect. 4.

3 Integrated Control/Structure Design (ICSD)

3.1 General Approach

Figure 6 shows the standard multi-channel $\mathscr{H}_\infty$ synthesis problem for ICSD of a generic system $G(s)$. The synthesis scheme is build by establishing the feedback of the *augmented* controller $K(s) = \text{diag}(C(s), \Delta)$ with the corresponding inputs/outputs of the nominal system $G(s)$. Additional channels are added in order to weight the controller's frequency response and mechanical performance index. The synthesis scheme has three different channels:

- One multidimensional channel which connects the perturbations of the system, w, to the performance outputs, z, through the weighting W_z.
- One multidimensional channel which connects the inputs of the control system, y_c, to the outputs, u_c, to shape the frequency-domain response of the controller $C(s)$ (roff-off behavior for instance) through the weighting W_C.

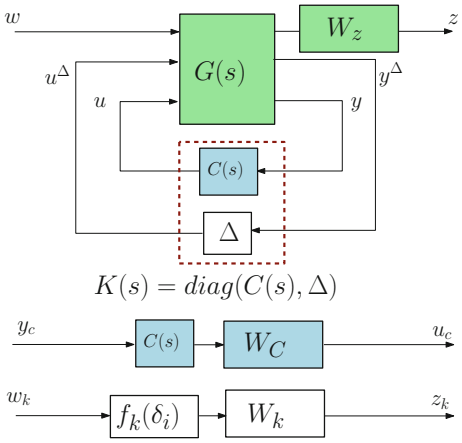

Fig. 6 Block diagram of integrated design optimization

- One multidimensional channel which connects the inputs w_k of the mechanical performance function $f_k(\delta_i)$ block to its outputs z_k, through a weighting W_k. This function $f_k(\delta_i)$ depends directly on the design parameters variations δ_i (i.e. the various independent components of the block Δ).

Structured $\mathscr{H}_\infty$ synthesis computes the sub-optimal tuning of the free parameters of $C(s)$ and Δ embedded in $K(s)$ to enforce closed-loop internal stability, $\mathscr{F}_l(G(s), K(s))$, such that:

$$\min_{K(s)} \{\max\{\|W_k(s) f_k(\delta_i)\|_\infty, \|W_C(s)C(s)\|_\infty\}\}$$

such that

$$\|W_z(s)T_{w\to z}(s)\|_\infty < \gamma_{perf}$$

i.e., it minimizes the $\mathscr{H}_\infty$ norm between the transfer of the perturbation input w and the performance output z, $T_{w\to z}(s)$, such that it is constrained to be below $\gamma_{perf} > 0$ to meet the required performances. The problem is in the form of multi-channel $\mathscr{H}_\infty$ synthesis, and it allows the set of desired properties to the augmented controller such as its internal stability [6], frequency template [17] or maximum gain values, while minimizing a mechanical performance index. In substance, the structured $\mathscr{H}_\infty$ integrated design synthesis tunes the free parameters contained in the augmented controller $K(s) = \text{diag}(C(s), \Delta_i)$ to ensure closed loop internal stability and meet normalized $\mathscr{H}_\infty$ requirements through W_z, W_C and W_k.

3.2 Application to the Rotatory Spacecraft

The augmented controller is formed by concatenating the block of tunable parameters Δ with the real controller of the system, $C(s)$. Since the Δ block has been defined in Sect. 2.3, the structure of $C(s)$ is addressed in this section.

The system needs to reject low frequency disturbances in the rigid body DOF, the system's rotation around the hub, and can be helped by inducing active damping through the piezoelectric laminate installed on appendage 1. Thus, the control system will consist of two decentralized loops: one for the rigid body rotation of the hub, θ_{hub}, and the other to damp the first appendage's tip vibrations, $\ddot{w}_{tip_1}$.

The control of the rigid body motion is achieved with a PD (Proportional-Derivative) controller to compute the control torque provided by the reaction wheel located at the hub. The active damping controller (Active: AF) will be a simple rate feedback, integrating the first appendage's vertical acceleration (acceleration feedback strategy). Therefore the control law is structured as follows:

$$\{u\} = [C(s)]\{y\} = \begin{Bmatrix} t_{hub} \\ v \end{Bmatrix} = \begin{bmatrix} k_v & k_p & 0 \\ 0 & 0 & k_a/s \end{bmatrix} \begin{Bmatrix} \dot{\theta}_{hub} \\ \theta_{hub} \\ \ddot{y}_{tip_1} \end{Bmatrix} \tag{5}$$

The proportional control gain k_p, the derivative control gain k_v and the damping gain k_a, together with the tunable parameters of the Δ block, are to be optimized with structured $\mathscr{H}_\infty$ synthesis. The values of the PD controller gains are initialized using the standard tuning assuming the spacecraft is rigid: $k_p = J_t\omega^2$ and $k_v = 1.4J_t\omega$ where J_t is the total inertia and ω the wanted attitude servo-loop bandwidth ($\omega =$ 1 rad/s leads to: $K_p = 633.33$ Nm and $k_v = 231.21$ Nms).

As previously specified, the control of the hub rotation must be able to reject low frequency disturbance torque. The desired closed-loop dynamics for perturbation rejection are $\omega = 1$ rad/s and $\xi = 0.7$, which leads to the following weighting filter on the Acceleration Sensitivity Function ASF [6] (i.e. transfer from $w(1) = w_{\ddot{\theta}_{hub}}$ to output $z(1) = \ddot{\theta}_{hub}$ in Fig. 4):

$$W_{\ddot{\theta}_{hub}}(s) = \frac{s^2 + 1.4\omega s + \omega^2}{s^2} = \frac{s^2 + 1.4s + 1}{s^2} \tag{6}$$

The damping of the flexible modes is imposed by a template on the transfer between the hub's acceleration disturbance $w(1) = w_{\ddot{\theta}_{hub}}$ and the performance output $z(2) = \ddot{w}_{tip}$. This template reads: $W_{\ddot{q}P}(s) = L/W_{\ddot{\theta}_{hub}}$ (L is the nominal length of the beam). A static filter $W_d = 1/M_{tot}$ (with M_{tot} the nominal total mass) is added in the transfer $f_{y,tip} \rightarrow \ddot{w}_{tip}$ to add additional damping. In Figs. 7 and 8 frequency-domain responses of the closed-loop transfers $T_{w(1)\rightarrow z(1)}$ (called hub's dynamics) and $T_{w(1)\rightarrow z(2)}$ (called tip's dynamics) when only the 2 gains k_p and k_v of the PD controller are optimized. These responses are compared with the desired frequency response imposed through the templates and $W^{-1}_{\ddot{\theta}_{hub}}(s)$ and $W_{\ddot{q}P}(s)$. It is seen that the

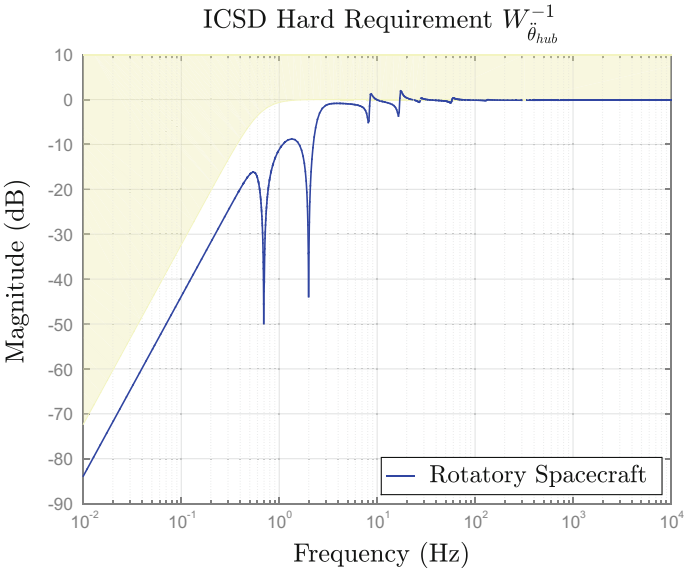

Fig. 7 Constraint (*yellow*) on the hub's dynamics (*blue*)

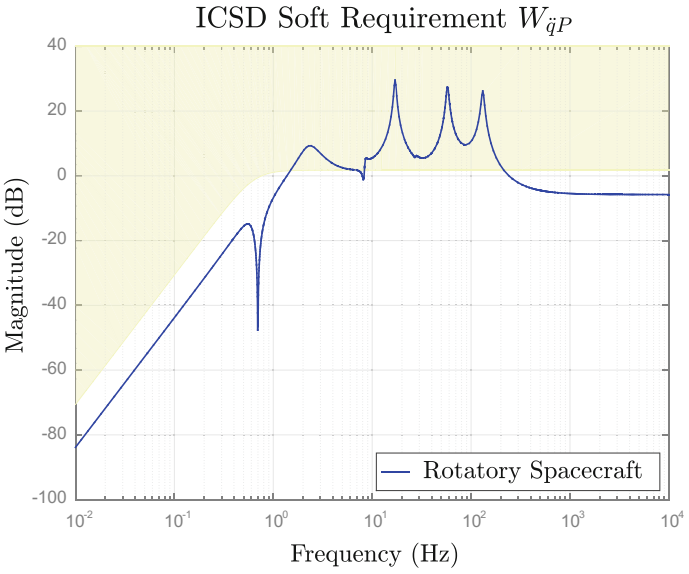

Fig. 8 Constraint (*yellow*) on the tip's dynamics (*blue*)

flexible modes are badly damped and the PD controller gains have a larger value than the needed to respect the template on the ASF of the hub position θ_{hub}.

Once the constraints for rigid and flexible motion have been defined, additional channels can be added to constraint the variation of structural parameters. The constraints for the maximization of the length and tip mass of appendage 1, L_1 and M_1 respectively, are implemented as follows:

$$f_{M_1}(\delta_{M_1}) = \frac{1}{1 + 0.3\delta_{M_1}}; \quad W_{M_1} = 0.75 \tag{7}$$

$$f_{L_1}(\delta_{L_1}) = \frac{1}{1 + 0.3\delta_{L_1}}; \quad W_{L_1} = 0.75 \tag{8}$$

where the W_k values have been fixed to 0.75, a value which can never be reached with the allowed maximal variation, in order to encourage the maximum possible value for δ_{L_1} and δ_{M_1}. The constraint for minimum total mass is:

$$f_{M_{total}}(\delta_{L_i}, \delta_{M_i}) = L\,\rho\,t\,h\,(4 + 0.3\sum_{i=1}^{4}\delta_{L_i}) + m_t(4 + 0.3\sum_{i=1}^{4}\delta_{M_i}); \quad W_{M_{total}} = M_0 \tag{9}$$

where $M_0 = 15.51\,\text{kg}$ is the nominal total mass of all the appendages. Equation (9) is a combination of all the structural parameters that can be varied, weighted by their impact on the system total mass (total beams mass for the lengths, total tip mass for the tip masses).

Finally, the ICSD problem can be summarized in the following way ($T_{i\to o}$ denotes the closed-loop transfer from input i to output o defined in the model of Fig. 4):

Find a stabilizing set of parameters $\Theta = \{k_v, k_p, k_a, \delta_{M_i}, \delta_{L_i}\}$ such that:

$$\begin{aligned}\min_{\Theta}\{\max\{\ & \|W_{M_1} f_{M_1}(\delta_{M_1})\|_\infty, \|W_{L_1} f_{L_1}(\delta_{L_1})\|_\infty, \\ & \|W_{M_{total}} f_{M_{total}}(\delta_{L_i}, \delta_{M_i})\|_\infty, \|W_{\ddot{q}P}^{-1}(s) T_{w(1)\to z(2)}(s)\|_\infty, \\ & \|W_d T_{w(2)\to z(2)}(s)\|_\infty\}\}\end{aligned}$$

under the constraint:

$$\|W_{\ddot{\theta}_{hub}}(s) T_{w(1)\to z(1)}(s)\|_\infty < 1.5.$$

4 Results

The optimization of the controller and the structural parameters is performed using the structured $\mathscr{H}_\infty$ synthesis tool *systune*. The results of the ICSD solution are compared with those of a solution with control optimization alone (COA). Table 2 shows the optimized and nominal structural parameters. It can be seen that the length and tip mass of appendage 1 have been increased the maximum allowed, 30%. For appendages 2, 3 and 4 the tip masses have been minimized while the lengths have been increased almost to the maximum, with the exception of appendage 2. Appendage 3 and its opposite appendage 4 are no longer symmetric since they lengths are slightly different and the tip masses difference is around 0.15 kg. The structural optimization meets the specifications: maximization of mass and length of appendage 1 while minimizing the impact on the total system's mass.

Figures 9 and 10 show the resulting frequency response for $T_{w(1)\to z(1)}$ and $T_{w(1)\to z(2)}$ compared with the desired templates $W_{\ddot{\theta}_{hub}}^{-1}$ and $W_{\ddot{q}P}$ after optimization. The gains of the PD controller have been adjusted to fit the frequency template and flexible modes are shifted and more damped when comparing with the response given in Figs. 7 and 8. The shift of flexible modes is a consequence of the structural optimization, since tip masses and lengths have been modified. The damping is provided by the active damping provided by the piezoelectric material controlled with an acceleration feedback control law.

The ICSD solution enjoys the same robust performance as the COA solution for the hub position control. The NICHOLS diagram of the open loop $t_{hub} \to t_{com}$ response in Fig. 11 shows that the ICSD solution has satisfactory phase and gain margins (GM = 20.5 dB, PM = 69.1°) which are as good as the COA solution (GM = 13.5 dB, PM = 69.1°). However, this is achieved by the ICSD solution with longer appendages which are not symmetric. Indeed, the first flexible mode, located at $\omega =$ 4.4 rad/s appears to be uncontrollable in nominal configuration, corresponding to the symmetric bending of the system's appendages. However, the ICSD solution has tuned the system to be completely asymmetric so that the first flexible mode can be governed with the hub torque as well. This is confirmed in Fig. 12, where the BODE diagram of the open loop response shows that the first flexible mode appears as a

Table 2 Structural data before optimization (COA) and after performing ICSD to the rotatory flexible spacecraft

Parameters	COA	ICSD
Controller	PD + AF	PD + AF
Lengths L_1 & L_2	1.22 m	$L_1 = 1.59$ m & $L_2 = 1.36$ m
Masses M_1 & M_2	2.29 kg	$M_1 = 2.98$ kg & $M_2 = 1.60$ kg
Lengths L_3 & L_4	1.22 m	$L_3 = 1.59$ m & $L_4 = 1.54$ m
Masses M_3 & M_4	2.29 kg	$M_3 = 1.75$ kg & $M_4 = 1.60$ kg
Total Appendages Mass	15.51 kg	15.83 kg

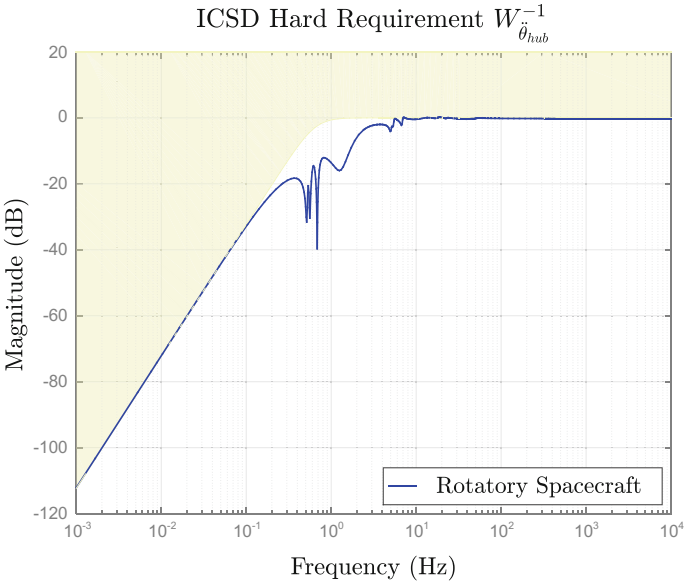

Fig. 9 Constraint (*yellow*) on the hub's dynamics (*blue*)

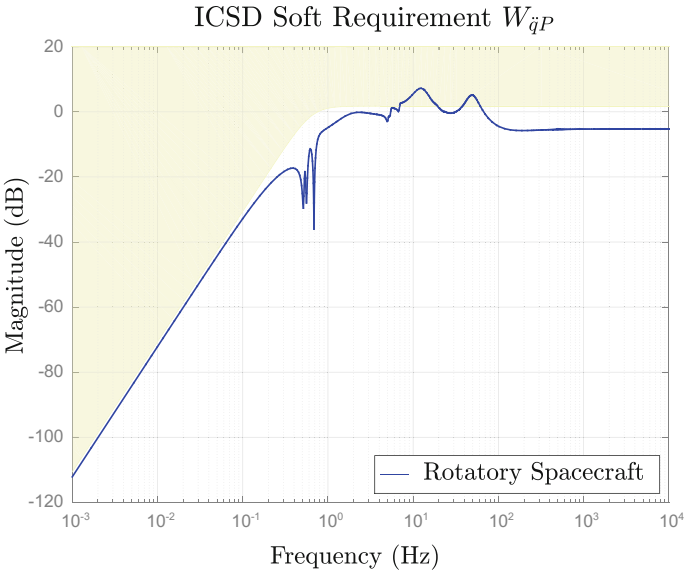

Fig. 10 Constraint (*yellow*) on the tip's dynamics (*blue*)

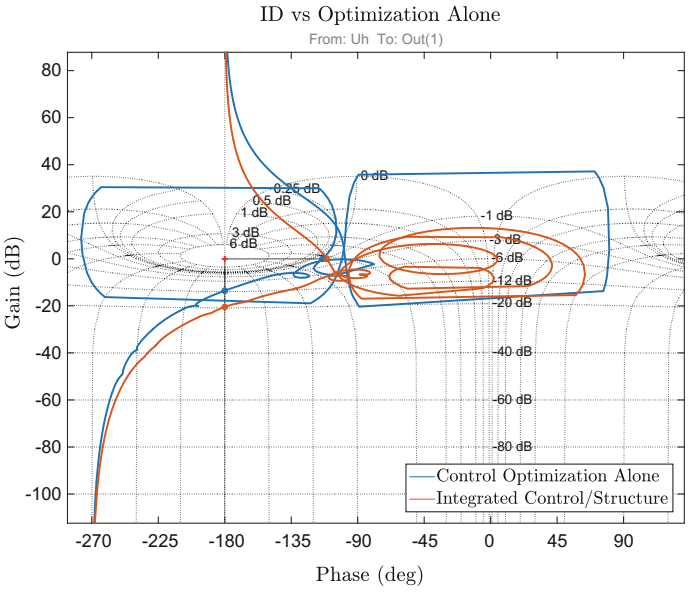

Fig. 11 NICHOLS plot

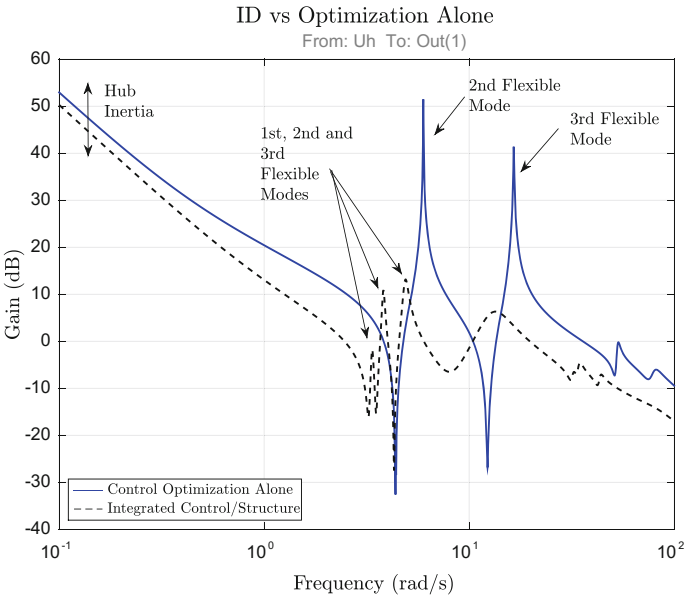

Fig. 12 BODE plot

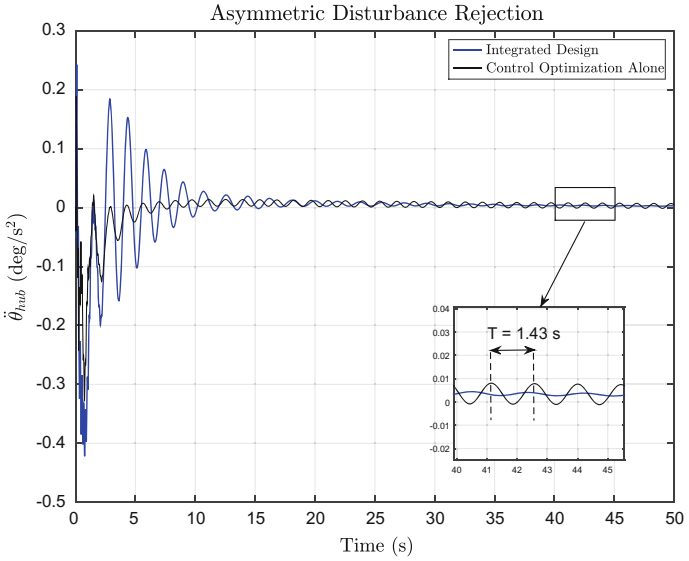

Fig. 13 Hub acceleration $\ddot{\theta}_{hub}$

resonance frequency in the ICSD solution and as an anti-resonance frequency for the COA solution.

The uncontrollability of the first symmetric bending mode at $\omega = 4.4$ rad/s is also verified in the time domain response. Figures 13 and 14 show the closed-loop response of the hub's acceleration $\ddot{\theta}_{hub}$ and the first appendage tip's acceleration $\ddot{y}_{tip_1}$, respectively, to an asymmetric torque disturbance at tips 1 and 3 and for both ICSD and COA solutions. This input excites the symmetric bending mode of appendages 3 and 4, which cannot be damped by the COA solution. It can be seen as well that the acceleration of the COA solution has a higher overshoot than the ICSD solution, even if the ICSD solution has higher tip mass and length. On the other hand, the ICSD solution needs two times more time for damping the tip vibrations and hub's position oscillations.

The results show that ICSD using structured $\mathscr{H}_\infty$ synthesis can be achieved by implementing the desired specifications in $\mathscr{H}_\infty$ form. The structured $\mathscr{H}_\infty$ synthesis optimizes the controller and the structural parameters to better fit the dynamic specifications, while respecting the structural constraints imposed to the varying parameters. The same level of performance can be achieved with a modified structure, discovering new configurations which can improve control performance. The optimization process has provided an intuitive fact: the maximization of the mass of one appendage will decrease the total mass of the others. The optimization has provided a counter-intuitive fact as well: system's asymmetry can help to increase controllability of system's modes and to improve system's performance. Therefore,

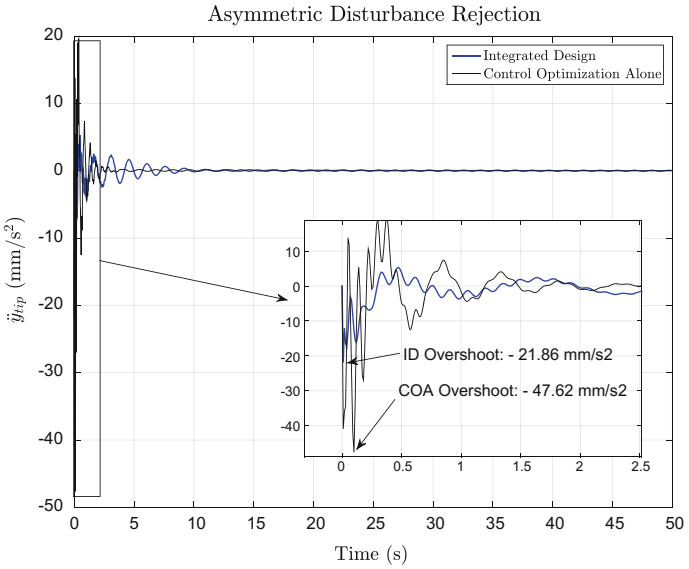

Fig. 14 Tip acceleration $\ddot{w}_{tip}$

integrated design is possible and it takes into account the issues and trade-offs of the physical system.

5 Conclusions and Perspectives

The implementation of dynamic, structural and controller specifications for the integrated control/structure design (ICSD) has been explained in this paper. The specifications for the rigid body motion are implemented weighting the Acceleration Sensitivity Function (ASF), while the flexible motion damping is achieved by projecting the rigid body motion template at different points of the Flexible Multi-body System (FMS). The structural constraints for structured optimization are implemented with additional channels which included the cost functions and weighting filters applied to the varying parameters involved in the constraints. Controller frequency shaping can be stated through a roll-off filter. The application of ICSD on a flexible planar rotatory spacecraft provided quite promising results. Further works will use the same approach to perform the ICSD of a more complex system, a flexible satellite, in the 3D case. The TITOP approach, used to obtain linear parameter varying models of flexible multi-body systems required for such a ICSD, will be extended to flexible multi-body systems with closed-loop kinematic mechanisms.

References

1. Onoda J, Haftka R (1987) An approach to structure/control simultaneous optimization for large flexible spacecraft. AIAA 25:1133–1138
2. Gilbert MG (1988) "Results of an Integrated Structure/Control Law design sensitivity analysis," Technical Report NASA TM-101517, NASA, NASA Langley Research Center, Hampton, VA 23665–5225, Dec 1988
3. Messac A, Malek K (1992) Control structure integrated design. AIAA J 30:2124–2131
4. Hiramoto K, Mohammadpour J, Grigoriadis K (2009) Integrated design of system parameters, control and sensor actuator placement for symmetric mechanical systems. In 48th IEEE conference on decision and control, Shanghai, China, Dec 2009
5. Cimellaro G, Soong T, Reinhorn A (2008) Optimal integrated design of controlled structures. In: 14th world conference on earthquake engineering, Beijing, China, Oct 2008
6. Alazard D, Loquen T, de Plinval H, Cumer C (2013) Avionics/Control co-design for large flexible space structures. In: AIAA guidance, navigation, and control (GNC) conference. Massachusetts, USA, Boston, Aug 2013
7. Gahinet P, Apkarian P (August 2011) Structured H-infinity synthesis using MATLAB. In: 18th IFAC world congress. Milano, Italy
8. Burke J, Henrion D, Lewis A, Overton M (2006) HIFOO a Matlab package for fixed-order controller design and $\mathscr{H}_\infty$ optimization. In: 5th IFAC symposium on robust control design, 2006
9. Alazard D, Perez JA, Loquen T, Cumer C (2015) Two-input two-output port model for mechanical systems. In: AIAA science and technology forum and exposition, Kissimmee, Florida, Jan 2015
10. Perez JA, Alazard D, Loquen T, Cumer C, Pittet C (2015) Linear dynamic modeling of spacecraft with open-chain assembly of flexible bodies for ACS/structure co-design. In: Advances in aerospace guidance, navigation and control, pp 659–678, Springer
11. Perez JA, Alazard D, Loquen T, Pittet C, Cumer C (2016) Flexible multibody system linear modeling for control using component modes synthesis and double-port approach. ASME J Dyn Syst Meas Control, 138
12. Murali H, Alazard D, Massotti L, Ankersen F, Toglia C (2015) Mechanical-attitude controller co-design of large flexible space structures. Advances in aerospace guidance, navigation and control. Springer, Berlin, pp 639–658
13. Perez JA, Alazard D, Loquen T, Pittet C (2016) Linear modeling of a flexible substructure actuated through piezoelectric components for use in integrated control/structure design. In: 20th IFAC symposium on automatic control in aerospace, 2016
14. Perez JA, Pittet C, Alazard D, Loquen T Integrated control/ structure design of a large space structure using structured $\mathscr{H}_\infty$ control. In: 20th IFAC symposium on automatic control in aerospace
15. Perez J, Pittet C, Alazard D, Loquen T, Cumer C (2015) A flexible appendage model for use in integrated control/structure spacecraft design. In: IFAC workshop on advanced control and navigation for autonomous aerospace vehicles. Seville, Spain
16. Junkins JL, Kim Y (1993) Introduction to dynamics and control of flexible structures. AIAA
17. Loquen T, de Plinval H, Cumer C, Alazard D (2012) Attitude control of satellite with flexible appendages: structured H-infinity approach. In: AIAA guidance, navigation, and control (GNC) conference, Mineapolis (Minesota), Aug 2012